Journal of Biomechanics 44 (2011) 150–155

Contents lists available at ScienceDirect

Journal of Biomechanics

journal homepage: www.elsevier.com/locate/jbiomech
www.JBiomech.com

Finite element model of subsynovial connective tissue deformation due to tendon excursion in the human carpal tunnel

Jacqueline Henderson, Andrew Thoreson, Yuichi Yoshii, Kristin D. Zhao, Peter C. Amadio, Kai-Nan An*

Orthopedic Biomechanics Laboratory, Division of Orthopedic Research, Mayo Clinic, 200 1st SW, Rochester, MN 55905, USA

ARTICLE INFO

Article history:
Accepted 6 September 2010

Keywords:
Carpal tunnel
Subsynovial connective tissue (SSCT)
Finite element analysis model

ABSTRACT

Carpal tunnel syndrome (CTS) is a nerve entrapment disease, which has been extensively studied by the engineering and medical community. Although the direct cause is unknown, in vivo and in vitro medical research has shown that tendon excursion creates microtears in the subsynovial connective tissue (SSCT) surrounding the tendon in the carpal tunnel. One proposed mechanism for the SSCT injury is shearing, which is believed to cause fibrosis of the SSCT. Few studies have reported quantitative observations of SSCT response to mechanical loading. Our proposed model is a 2-D section that consists of an FDS tendon, interstitial SSCT and adjacent stationary tendons. We believe that developing this model will allow the most complete quantitative observations of SSCT response to mechanical loading reported thus far. Boundary conditions were applied to the FEA model to simulate single finger flexion. A velocity was applied to the FDS tendon in the model to match loading conditions of the documented cadaver wrist kinematics studies. The cadaveric and FEA displacement results were compared to investigate the magnitude of stiffness required for the SSCT section of the model. The relative motions between the model and cadavers matched more closely than the absolute displacements. Since cadaveric models do not allow identification of the SSCT layers, an FEA model will help determine the displacement and stress experienced by each SSCT layer. Thus, we believe this conceptual model is a first step in understanding how the SSCT layers are recruited during tendon excursion.

1. Introduction

Carpal tunnel syndrome (CTS) is a nerve entrapment disease, which has been extensively studied by the ergonomics and medical community (Armstrong and Chaffin, 1979; Luopajarvi et al., 1979; Armstrong et al., 1984; Amadio, 1987, 1992, 1995; Silverstein et al., 1987; Liberty, 2008). While the direct cause of CTS is unknown, in vivo and in vitro medical research has shown that tendon excursion creates microtears in the subsynovial connective tissue (SSCT) surrounding the tendon in the carpal tunnel (Cobb et al., 1992; Ettema et al., 2007; Zhao et al., 2007). These microtears are thought to initiate fibrosis of the SSCT, which creates a thickening of the SSCT layers, an increase in volume and an elevation in the carpal tunnel pressure, thus leading to a compression on the median nerve and leading to idiopathic CTS (Armstrong et al., 1984; Szabo and Chidgey, 1989; Cobb et al., 1992; Ettema et al., 2006a,b, 2007; Zhao et al., 2007).

1.1. Carpal tunnel and subsynovial connective tissue

Contained within the human carpal tunnel by the transverse carpal ligament are the median nerve, flexor pollicis longus (FPL), four flexor digitorum profundus (FDP) tendons and flexor digitorum superficialis (FDS) tendons. Connecting and surrounding these tendons and median nerve is the SSCT (Cobb et al., 1992). The SSCT is best described as multiple layers of collagen that surround the flexor tendons in the carpal tunnel. This layered matrix fills the region between and connects to the visceral synovial layer, flexor tendons and the median nerve within the carpal tunnel. Each layer is connected to adjacent layers by small fibrils (Cobb et al., 1992; Rotman and Donovan, 2002; Ettema et al., 2006a,b).

Subject to scientific evaluation, Guimberteau was one of the first to explain the shearing behavior of the SSCT, describing how the tendons within the carpal tunnel slide in this matrix during tendon excursion (Guimberteau, 2001). He hypothesized that as a layer shears past another, the fibrils connecting the layers behave similar to rubber cables; they can stretch, but not indefinitely. In addition, he hypothesized that the fibers become longer and thinner while stretching, but once these fibrils reached their maximum length, they transfer more load and recruit the adjacent layer and attached fibers. This process continues during

* Corresponding author. Tel.: +1 507 538 1717; fax: +1 507 284 5392.
E-mail address: an.kainan@mayo.edu (K.-N. An).

0021-9290/$ - see front matter © 2010 Elsevier Ltd. All rights reserved.
doi:10.1016/j.jbiomech.2010.09.001

tendon excursion until all layers are recruited. Thus, it was believed that fibers furthest from the tendon were not involved during tendon excursion.

Ettema et al. (2006a,b) were able to identify, through electron microscopy, the multiple layers of the SSCT and revealed that the SSCT layers ran parallel to the tendon and were interconnected by smaller fibrils. This model was further demonstrated experimentally. In documenting this motion, it was reported that the normal specimen's SSCT moved with a smooth motion separate from the tendon. This investigation determined that when the tendon moves, the fibrils connected to the tendon are set into motion first, followed by the fibrils connected to the paratenon layers, a pattern that propagated until the visceral synovium moved (Ettema et al., 2007).

The introduction of the gliding system SSCT model stimulated several studies to further investigate the relationship between the SSCT shear and tendon excursion, and whether this relationship may be influenced by pathology. Ettema et al. (2006a,b, 2007) determined that the motion of the FDS III tendon pulled the visceral synovium (VS) only after shearing of the SSCT.

1.2. Mechanical response

As early as the 1960s, various biomechanical models of the human hand were developed (Landsmeer, 1961a,b; Harris et al., 1966). Although anthropometrics may be important in understanding the human carpal tunnel, it was observed that the anatomical locations of the tendons are affected by wrist flexion and extension. Thus, the rate of tendon displacement for the flexor digitorum superficialis (FDS) was greater than that of the flexor digitorum profundus (FDP) tendon (Armstrong and Chaffin, 1978).

One proposed mechanism for the genesis of fibrosis of the SSCT is shear injury (Moore et al., 1991). Instead of reporting the relative motion of the tendon, SSCT and nerve, Yoshii et al. (2008) compared these motions using their shear strain index (SSI).

1.3. Mechanical and material properties of SSCT

Developing a model requires knowledge about the mechanical properties of the SSCT. Osamura et al. (2007) performed one of the earliest investigations on the mechanical properties of the SSCT. The shear-loaded mechanical test of the cadaveric SSCT without a medical history of CTS had a thickness of 0.48 mm and a shear modulus of 2.7 kPa.

1.4. Mathematical modeling

Although finite element studies have been used to explore mechanical insult to the median nerve and changes to the transverse carpal ligament, finite element analysis has not been used to analyze the relationship between the tendon excursion and SSCT deformation (Ko and Brown, 2007; Xin et al., 2007). Since the tools for evaluating the SSCT and tendon are limited, we aimed to develop a way to first understand the mechanics of the solid portion of a system, which consists of both solid and fluid components. This model allowed exploration of the feasibility of using a finite element analysis (FEA) model to describe the behavior of the deformation and displacement of the normal, non-fibrotic SSCT due to the excursion of tendon. More specifically, we tested the ability of the model to predict the SSCT deformation and validate it with experimental cadaveric measurements.

Up to this time there have been relatively few studies that have reported quantitative observations of SSCT response to mechanical loading. A basic model tuned to those observations, which have been reported can later be expanded to include other factors that can reasonably be expected to influence the mechanical response. These factors include microstructure of the tissue, geometry of the entire carpal tunnel structure, tissue pathology, wrist position and the role of fluid. Thus, this model will evolve along two paths from its current state, one which should result in increasingly accurate modeling of global relationships between SSCT and tendon, and the other, which could model local damage in the tissue. The model proposed in this work, a 2-D section consisting of a tendon, interstitial SSCT and carpal tunnel wall, was developed to allow use of the most complete quantitative observations of this structure that have been reported thus far.

2. Methods

2.1. Cadaveric observation through in vitro investigation

In designing the initial model, raw data acquired in the author's lab for previous studies, but not reported in the literature, was used for validation. The methods for collecting this data are described in detail in the previously published studies (Yoshii et al., 2008, 2009). A summary of these methods is warranted and followed. Ten thawed, fresh-frozen human cadaver hands were amputated approximately 15 cm proximal to the wrist joint. After creating a 5 mm diameter window in the flexor retinaculum, metal markers were embedded in the FDS of the middle finger and median nerve and glued to the SSCT and flexor retinaculum. Dacron cords were connected between the proximal ends of the FDS finger tendons and a mechanical actuator, and a resistance load of 100 g was attached to the distal tip of each finger. The actuator pulled the FDS tendons together proximally at a rate of 2.0 mm/s for 20 s. Fluoroscopic imaging was used to capture the lateral projection of the marker motion (Fig. 1). A custom MATLAB program converted the marker motion in the fluoroscopic projection into time dependent Cartesian coordinates. Testing was repeated for different wrist flexion/extension positions. For the purposes of this study, data for the neutral wrist posture were considered.

2.2. Model development

A symmetrical, 2-D conceptual model representing a longitudinal, cross-sectional slice of the carpal tunnel was developed to represent how tendon excursion deforms the SSCT. However the model is assumed to be applicable to a neutral wrist posture and results will be compared to the neural wrist position kinematics data obtained in the previous cadaveric studies. MSC.Patran MD R 2.1 software (MSC Software Corp, Santa Ana, CA) was used for pre-processing and meshing and Abaqus 6.6-1 software (Dassault Systemes, Lowell, MA) was used for

Fig. 1. Fluoroscopic image example with marker locations at initial and final position. (1—tendon; 2—SSCT).

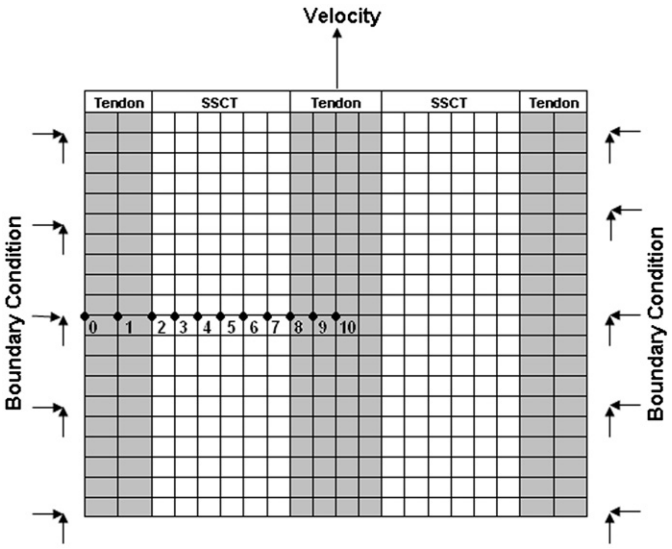

Fig. 2. Location of tendon and SSCT in FEA Model with boundary conditions.

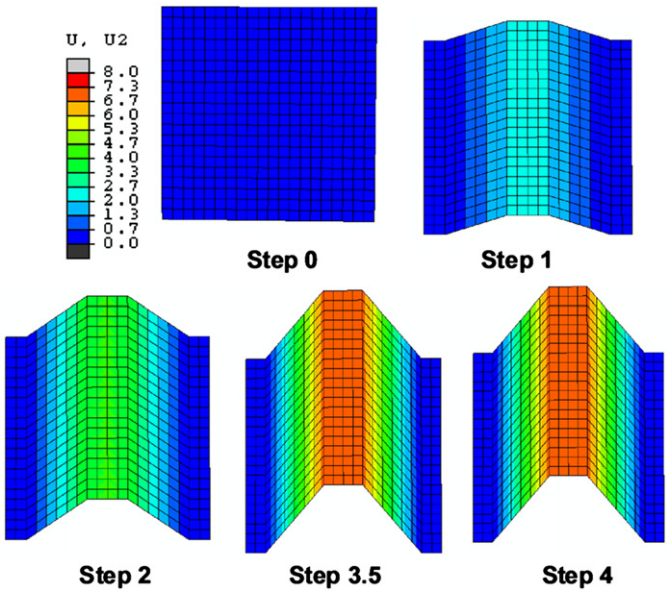

Fig. 3. Temporal longitudinal displacement of tendon and SSCT.

Table 1
Model parameters.

Component	Element type	Number of nodes	Elastic modulus (Mpa)	Poisson ratio
Tendon	Linear quadrilateral shell	351	0.27	0.2
SSCT	Linear quadrilateral shell	574	0.0027	0.2

analysis and post-processing. This conceptual model includes a complete FDS tendon surrounded on each side by SSCT tissue components, which in turn are grounded to stationary tendon surfaces (Fig. 2). Components were meshed uniformly with 4-node linear quadrilateral elements. The center tendon width, which represented the FDS tendon subjected to excursion during finger flexion, was 0.4 mm. Each stationary tendon section was 0.2 mm wide. The interstitial SSCT sections were 0.6 mm. These measurements were obtained by measuring a cross-sectional tendon and SSCT area of a human carpal tunnel.

Since the SSCT material properties and elastic modulus are not well characterized, findings of Osamura et al. (2007) were used as a general guide to determine the properties of the SSCT. They determined that the SSCT had a shear modulus of elasticity of 2.7×10^{-3} MPa. While further data is not available, we have chosen to assume that the normal SSCT behaves like a linear-elastic material. Additionally, since the tendon is known to be significantly stiffer than the SSCT, for the purpose of this study it was assumed that the tendon was 100 times stiffer than the SSCT. An elastic modulus of 2.7×10^{-1} MPa was applied to the tendon sections (Table 1).

2.3. Loading and boundary conditions

Boundary conditions were applied to the FEA model to simulate single finger flexion. A no-slip boundary condition was applied to the longitudinal outer faces of the left and right (stationary) tendons. A longitudinal velocity of 2 mm/s, the velocity applied by the linear actuator in the cadaver study, was applied to the center tendon for the duration of 4 s. Fig. 2 illustrates all boundary conditions applied to the model.

Validation for this FEA static model analysis was performed. Displacement of the tendon and SSCT were compared with those measured from cadaveric specimens using fluoroscopy. Displacements of the marker within the FDS tendon and on the SSCT were of greatest interest in this study. While we were not able to determine exactly what layer of SSCT the marker was attached to, we will assume that it lies near the middle of the thickness of the SSCT.

3. Results

In the FEA results, the displacement and the propagated shearing response was observed in this model (Fig. 3). The displacement of each node along the horizontal midline (one-half of the model is shown due to symmetry) was also plotted for each time step over the 4 s duration (Fig. 4). The orange area represents the SSCT and the purple area represents the tendon. Displacement is always zero at the left side where the no-slip boundary condition was applied and at a maximum at the FDS tendon center. Displacement of the mid-SSCT (node 5) and the tendon center (node 10) were used for comparison to cadaveric findings.

Selection of the reference nodes to characterize SSCT displacement is tied to our assumption that the marker in the referenced cadaver data was lodged mid-thickness in the SSCT. Maximum displacements observed in the tendon and SSCT reference nodes were 8 and 4 mm, respectively.

The cadaver marker motion was the standard for comparison. The displacement of each marker was averaged over the 10 specimens at each time point. The representative tendon and SSCT node displacement data was compared to the cadaveric tendon and SSCT marker displacement. The absolute displacement results between the cadaver and model are compared in Fig. 5.

Shear deformation of the SSCT as the tendon is displaced was the major focus of this model. Relative motion between the tendon and adjacent SSCT can quantify shear in the material. Therefore, relative motion was calculated for the cadaveric and FEA data (1). The relative motion of the FEA model was approximately 25% greater than the cadaveric findings at all time points (Fig. 6).

$$\text{Relative motion} = \text{Tendon displacement-SSCT displacement} \quad (1)$$

4. Discussion

The purpose of this model was to conceptually understand the interactions between the tendon and SSCT tissue during single digit tendon excursion and to match the ratio of deformation of the SSCT and tendon with experimental observations reported in the literature. Additionally, we used the findings reported by Yoshii et al. to validate our model. In developing this model we looked to demonstrate the deformation of the SSCT during tendon excursion, which is thought to lead to fibrosis of the SSCT and in turn potentially progress to CTS. Selection of a linear-elastic

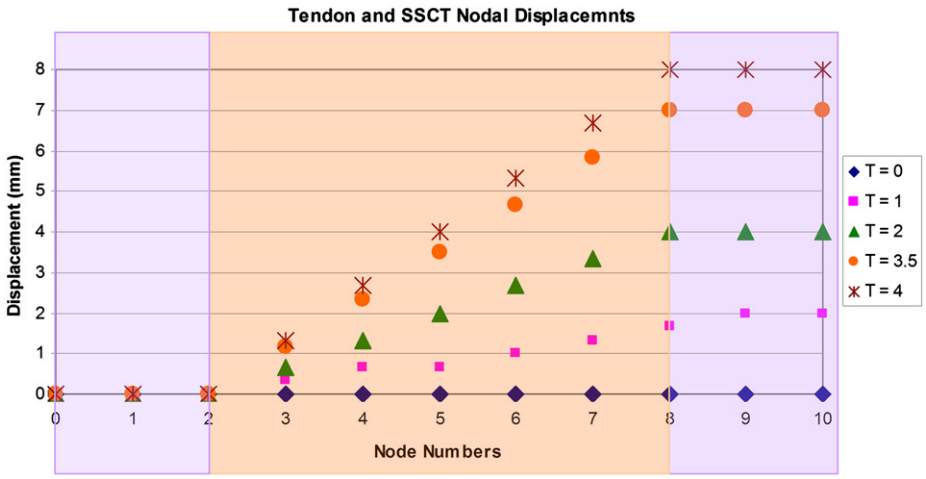

Fig. 4. Temporal nodal displacement of one-half of symmetrical model.

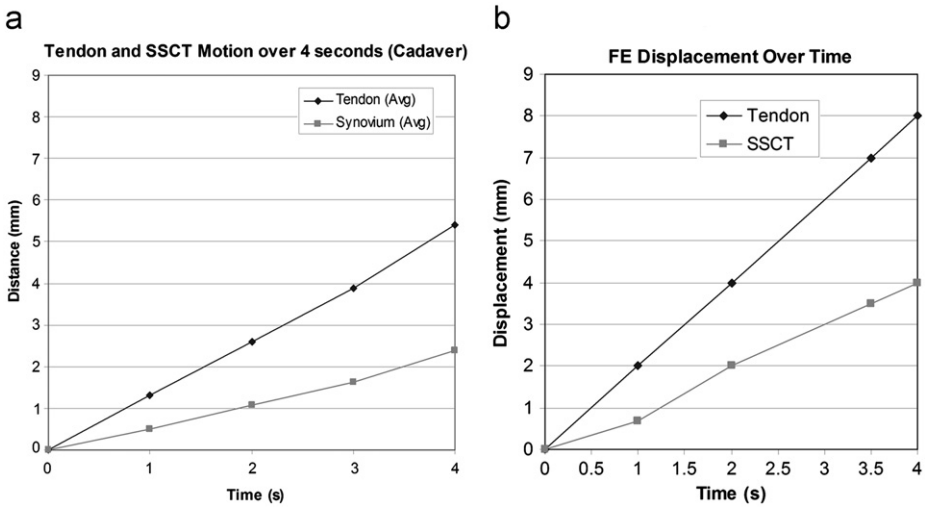

Fig. 5. (a and b) Cadaveric data vs. conceptual model.

material seemed to be appropriate as previous investigators have described SSCT with elastic properties (Osamura et al., 2007).

The cadaveric and FEA results were compared to investigate the magnitude of stiffness required for the SSCT section of the model. A modulus was selected based on the most complete mechanical testing of the SSCT reported to this point. If the modulus was close to the actual value, the relative motion between the tendon and SSCT in the FEA model and the cadaver study should be similar. Fig. 6 shows similar profiles between the two sets of results, but the displacement of the model are higher than the cadaver at all time points. The stiffness of material is dependent on two parameters: the modulus of elasticity and thickness. Knowing this, we calculated the relative motion of each node over 4 s. The relative motions between the data were more similar than the absolute displacements. Since relative motion in the FEA model was larger than was observed in the cadaver results, we initially concluded that either the modulus needs to be slightly decreased, or the space between the SSCT marker and the tendon in the cadaver model is smaller than that represented in the model. After further investigation, there was a 25% difference between the FEA model and the results reported by Yoshii et al. This difference can be explained by our choice of material properties, the limited knowledge of the SSCT marker placement or an acceleration of the actuator to reach the 2 mm/s velocity.

A consequence of selecting a linear-elastic material for this model is that the structure can stretch and return to its original size and shape without permanent deformation. True behavior of the carpal tunnel structure may not be so simple and may be further complicated through development of fibrosis in the SSCT.

We believe the FEA model can be used to represent in vivo and in vitro results. The use of a cadaveric model does not allow for us to identify the SSCT layers and their motion, but the use of FEA will help us determine the stress experienced by each layer in the SSCT. Thus, it can be stated that this conceptual model is potentially a beginning to understanding how the SSCT layers are recruited during tendon excursion.

Comparing the shear strain index in the carpal tunnel, the neutral posture was the assumed position of this model. We recognize that the posture of the hand and wrist is an important factor in the development and observation of symptoms of CTS (Marras and Schoenmarklin, 1993). Therefore, compression caused by wrist flexion, extension or the development of fibrotic SSCT within the carpal tunnel was not considered in this feasibility model.

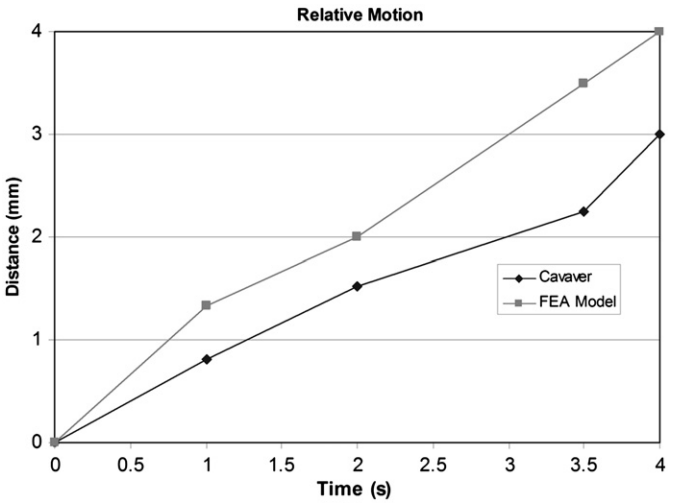

Fig. 6. Relative motion of cadaveric data vs. relative motion of conceptual model.

This study has several limitations, most of which can be overcome as improved in vivo or ex vivo modeling techniques for evaluating carpal tunnel biomechanics are reported. Since the distance between the SSCT layers is small, control of SSCT marker placement during specimen preparation is difficult as is determining its position within the interstitial space. The fluoroscopic data could only capture components of the marker motion in the plane of the image, and any perpendicular motion component may result in an underestimate of total motion. The referenced cadaver study collected tendon data in active loading mode while in flexion. Deformation of the cadaver SSCT when the load was released was not determined. Such evaluation may reveal information regarding visco-elastic properties of the SSCT. This study also only compared FEA results to data generated from cadavers with no history of CTS. Inclusion of wrist specimens with a history of CTS in a biomechanical and histological study may confirm that a key difference exists in the SSCT deformation. In this study, the SSCT section of the FEA model is assumed to be a homogeneous, isotropic mass. Histologic evaluation tells us otherwise, but the assumption was explored in this model to determine a target equivalent stiffness of the SSCT structure, towards which future, microstructural models will be challenged to match. However, an SSCT with fibrosis will change the stress distribution and material properties of the structure (Ettema et al., 2004, 2006a,b).

Unfortunately, the mechanical properties of the SSCT have not been well-documented; thus further insight is needed. As a conceptual model, more investigation with respect to the SSCT layers and how each layer is affected by tendon excursion of normal subjects is needed. The use of ultrasound or other imaging techniques will provide additional information for the development of this model. Narrowing the scope to an FEA model of a group of SSCT layers is needed to further understand how load is transferred. In future studies, the model can be developed to determine the stress distribution generated in the SSCT, which in turn will lead to a greater understanding of how fibrotic SSCT develops. Clearer understanding of SSCT stress and deformation will explain how it may lead to the fibrosis seen in CTS patients.

Since our ultimate goal of modeling the human carpal tunnel is to calculate the stress of the SSCT and the potential location of the microtear, which leads the fibrosis that compresses the nerve in a person diagnosed with CTS, we believe that this conceptual model is the best way to begin understanding these stresses.

Conflict of interest statement

The authors confirm that there is no potential conflict of interest including employment, consultancies, stock ownership, honoraria, and paid expert testimony, and patent applications influencing this work.

Acknowledgments

This project was supported by NIH Grant number 5T32HD007447-17, NICHD.

References

Amadio, P.C., 1987. Carpal tunnel syndrome, pyridoxine, and the work place. Journal of Hand Surgery [Am] 12 (5 Pt 2), 875–880.
Amadio, P.C., 1992. The Mayo Clinic and carpal tunnel syndrome. Mayo Clinic Proceedings 67 (1), 42–48.
Amadio, P.C., 1995. An epidemiologic study of carpal tunnel syndrome and hand-arm vibration syndrome in relation to vibration exposure [comment]. Journal of Hand Surgery [Am] 20 (2), 345–346.
Armstrong, T.J., Castelli, W.A., Evans, F.G., Diaz-Perez, R., 1984. Some histological changes in carpal tunnel contents and their biomechanical implications. Journal of Occupational Medicine 26 (3), 197–201.
Armstrong, T.J., Chaffin, D.B., 1978. An investigation of the relationship between displacements of the finger and wrist joints and the extrinsic finger flexor tendons. Journal of Biomechanics 11 (3), 119–128.
Armstrong, T.J., Chaffin, D.B., 1979. Carpal tunnel syndrome and selected personal attributes. Journal of Occupational Medicine 21 (7), 481–486.
Cobb, T.K., Dalley, B.K., Posteraro, R.H., Lewis, R.C., 1992. The carpal tunnel as a compartment. An anatomic perspective. Orthopaedic Review 21 (4), 451–453.
Ettema, A.M., Amadio, P.C., Zhao, C., Wold, L.E., An, K.N., 2004. A histological and immunohistochemical study of the subsynovial connective tissue in idiopathic carpal tunnel syndrome. Journal of Bone & Joint Surgery [Am] 86-A (7), 1458–1466.
Ettema, A.M., Amadio, P.C., Zhao, C., Wold, L.E., O'Byrne, M.M., Moran, S.L., et al., 2006a. Changes in the functional structure of the tenosynovium in idiopathic carpal tunnel syndrome: a scanning electron microscope study. Plastic & Reconstructive Surgery 118 (6), 1413–1422.
Ettema, A.M., Belohlavek, M., Zhao, C., Oh, S.H., Amadio, P.C., An, K.N., 2006b. High-resolution ultrasound analysis of subsynovial connective tissue in human cadaver carpal tunnel. Journal of Orthopaedic Research 24 (10), 2011–2020.
Ettema, A.M., Zhao, C., Amadio, P.C., O'Byrne, M.M., An, K.N., 2007. Gliding characteristics of flexor tendon and tenosynovium in carpal tunnel syndrome: a pilot study. Clinical Anatomy 20 (3), 292–299.
Guimberteau, J.C., 2001. New Ideas in Hand Flexor Tendon Surgery the Sliding System. Vascularized Flexor Tendon Transfers. Aquitaine Domaine Forestier, France.
Harris, E.H., Walker Jr, L.B., Bass, B.R., 1966. Stress–strain studies in cadaveric human tendon and an anomaly in the Young's modulus thereof. Medical & Biological Engineering 4 (3), 253–259.
Ko, C., Brown, T.D., 2007. A fluid-immersed multi-body contact finite element formulation for median nerve stress in the carpal tunnel. Computer Methods in Biomechanics & Biomedical Engineering 10 (5), 343–349.
Landsmeer, J.M., 1961a. Studies in the anatomy of articulation. I. The equilibrium of the "intercalated" bone. Acta Morphologica Neerlando-Scandinavica 3, 287–303.
Landsmeer, J.M., 1961b. Studies in the anatomy of articulation. II. Patterns of movement of bi-muscular, bi-articular systems. Acta Morphologica Neerlando-Scandinavica 3, 304–321.
Liberty Mutual, 2008. Liberty Mutual Workplace Safety Index. 〈http://www.libertymutualgroup.com〉 (retrieved May 1, 2009).
Luopajarvi, T., Kuorinka, I., Virolainen, M., Holmberg, M., 1979. Prevalence of tenosynovitis and other injuries of the upper extremities in repetitive work. Scandinavian Journal of Work, Environment & Health 5 (Suppl. 3), 48–55.
Marras, W.S., Schoenmarklin, R.W., 1993. Wrist motions in industry. Ergonomics 36 (4), 341–351.
Moore, A., Wells, R., Ranney, D., 1991. Quantifying exposure in occupational manual tasks with cumulative trauma disorder potential. Ergonomics 34 (12), 1433–1453.
Osamura, N., Zhao, C., Zobitz, M.E., An, K.N., Amadio, P.C., 2007. Evaluation of the material properties of the subsynovial connective tissue in carpal tunnel syndrome. Clinical Biomechanics 22 (9), 999–1003.
Rotman, M.B., Donovan, J.P., 2002. Practical anatomy of the carpal tunnel. Hand Clinics 18 (2), 219–230.
Silverstein, B.A., Fine, L.J., Armstrong, T.J., 1987. Occupational factors and carpal tunnel syndrome. American Journal of Industrial Medicine 11 (3), 343–358.
Szabo, R.M., Chidgey, L.K., 1989. Stress carpal tunnel pressures in patients with carpal tunnel syndrome and normal patients. Journal of Hand Surgery [Am] 14 (4), 624–627.
Xin, G., Yubo, F., Zong-Ming, L., 2007. Three dimensional finite element analysis on the morphological change of the transverse carpal ligament. In: Proceedings of

the IEEE/ICME International Conference on Complex Medical Engineering, 2007, CME 2007.
Yoshii, Y., Zhao, C., Henderson, J., Zhao, K.D., An, K.N., Amadio, P.C., 2009. Shear strain and motion of the subsynovial connective tissue and median nerve during single-digit motion. Journal of Hand Surgery [Am] 34 (1), 65–73.
Yoshii, Y., Zhao, C., Zhao, K.D., Zobitz, M.E., An, K.N., Amadio, P.C., 2008. The effect of wrist position on the relative motion of tendon, nerve, and subsynovial connective tissue within the carpal tunnel in a human cadaver model. Journal of Orthopaedic Research 26 (8), 1153–1158.
Zhao, C., Ettema, A.M., Osamura, N., Berglund, L.J., An, K.N., Amadio, P.C., 2007. Gliding characteristics between flexor tendons and surrounding tissues in the carpal tunnel: a biomechanical cadaver study. Journal of Orthopaedic Research 25 (2), 185–190.